JETIR.ORG ISSN: 2349-5162 | ESTD Year : 2014 | Monthly Issue
JOURNAL OF EMERGING TECHNOLOGIES AND INNOVATIVE RESEARCH (JETIR)
An International Scholarly Open Access, Peer-reviewed, Refereed Journal

Exploring Solar Dynamics Using Advanced Astronomy Tools: Analysis of Sunspot Evolution Using High-Resolution Data

Darsh Nayak, Sujal Prajapati, Dr. Ayushi Patel
Department of Physics, Indus Institute of Sciences, Humanities and Liberal Studies, Indus University,
darshnayak.22.phy@ishls.indusuni.ac.in
Department of Physics, Indus Institute of Sciences, Humanities and Liberal Studies, Indus University,
sujalprajapati.22.phy@ishls.indusuni.ac.in
Department of Physics, Indus Institute of Sciences, Humanities and Liberal Studies, Indus University ,
ayushipatel.ishls@indusuni.ac.in

***ABSTRACT*—Sunspots are dark, magnetically active regions on the Sun's photosphere, formed due to intense and varying magnetic fields that inhibit the escape of light from the Sun's interior. Their behavior is critical to understanding solar dynamics and forecasting space weather phenomena. In this study, a predictive model is developed to estimate the positional movement of sunspots over time, using their observed distances from the solar limb. The model employs polynomial regression, offering a balance between computational simplicity and predictive accuracy. High-resolution data spanning 7 to 10 days was extracted from imagery captured by NASA's Solar Dynamics Observatory (SDO), specifically using the HMIIC filter. Despite the nonlinear and complex nature of solar phenomena, the model demonstrates strong predictive capabilities over extended periods. It accurately forecasts sunspot displacements up to approximately 384–410 hours (about 16–17 days), with a coefficient of determination (R^2) consistently exceeding 0.95. This approach integrates thorough feature testing, polynomial degree optimization, and robust error analysis. The results show a high correlation between predicted and actual sunspot positions, validating the effectiveness of polynomial regression in short-term solar activity prediction. The study contributes a novel tool for real-time solar monitoring and enhances understanding of sunspot dynamics using limited yet high-quality observational data.**

***Keywords*—sunspots, polynomial regression, distance, velocity, solar dynamics**

I. INTRODUCTION

Sun, the powerhouse of the entire Solar System and nearest star to Earth, is situated at the center of our Solar System and holds every planet, rocks icy and gaseous objects in it with the strength of its gravity. Its energy comes from its core, a huge nuclear reactor, where hydrogen atoms convert into helium atom through the process of nuclear fusion [1]. This leads to a release of extensive amounts of radiation and light energy for itself and a majority of ours as well. The Sun's age is approximated to be somewhere around 4.6 billion years old [2], [3], which was established by the process of radiation dating some of the oldest meteors residing in our universe. The Sun is considered a G2V type star, which means that it is a G-type main sequence [1] star of second sub-class with a surface temperature of around 5,800 Kelvin [4], [5]. According to Population classification, which classifies the stars according to the colour (temperature) and their population, the Sun is a Population I or Pop-I star [4], [6]. The Sun is wrongly believed as a yellow dwarf, since the light released by the Sun is actually white. The Sun releases a steady stream of charged particles through its powerful eruptions, Solar wind, Solar flares and Coronal Mass Ejections (CMEs), influences the space weather in the Solar system [10].

Each second, the Sun goes through nuclear fusion of about 600 million tons of hydrogen which then turns into helium, resulting in 4 million tons of matter to turn into energy [11]. The energy created, can take a time period of approximately 10,000 to 170,000 years to escape the core.

TABLE I. SOME IMPORTANT PARAMETERS OF THE SUN [5-9]

Parameters of the Sun	***Values***
Type	G2V (Population-I, according to Population Classification)
Age	4,500,000,000 years
Diameter	1.39 x 10^6 kilometers
Radius	6.957 x 10^5 kilometers [9]
Surface Temperature	≈ 5,778 K

Parameters of the Sun	*Values*
Core Temperature	≈ 15,000,000 K
Mass	1.989 x 10^{30} kilograms
Surface Area	6.0877 x 10^{12} km^2
Circumference	4.36 x 10^6 kilometers
Average distance between Sun and Earth	1.496 x 10^8 kilometers
Average distance between Sun and Oort Cloud (outermost edge of the Solar System)	1.49598 x 10^{13} to 2.991957 x 10^{13} kilometers
Pressure	2.477 x 10^{11} bar
Density	1.622 x 10^5 kg/m^3
Luminosity	3.828 x 10^{26} J/s or W [9]
Magnetic field strength	At Sunspots:2000-3000 Gauss Active regions:100-300 Gauss
Magnetic field's reach (Heliosphere)	1.795 x 10^{10} kilometers

From Earth, the Sun appears to be an unchanging source of light and heat in the sky, but it is a dynamic star that continually changes and emits energy into space [12]. Studying the Sun allows us to predict and mitigate the effects of space weather, which can disrupt [12]: Satellite communications and navigation systems (GPS), Power grids, leading to widespread blackouts, Radio communications, Astronaut safety in space.

The thickness of photosphere is about tens to hundreds of kilometers, and is slightly less opaque than air on Earth [13]. The upper part of the photosphere is cooler than the lower part, which leads to the Sun appearing brighter at the center and dimmer towards the edge or limb of the Solar disk. This phenomenon is known as limb darkening [13]. Sunlight radiates at an approximate temperature of 5,778 K, and has a similar spectrum of a black-body [14]. Norman Lockyer postulated in 1868 that a new element, which he named helium after the Greek Sun deity Helios, was the source of these absorption lines. Twenty-five years later, helium was isolated on Earth [15].

Though the corona and Solar wind has an average temperature of about 1,000,000 – 2,000,000 K [10]; the temperature in the hottest regions can reach to 8,000,000 – 20,000,000 K. Sunspots are temporary spots on the Sun's surface that appear darker than the surrounding areas [12], [16]. They are one of the most recognizable Solar phenomena and can usually affect the entire Solar atmosphere. They appear as black/dark spots on the Photosphere in variable shapes and sizes [16].

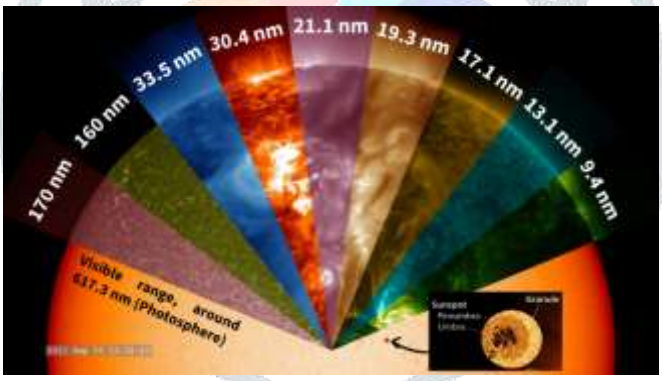

Fig. 1. Image of sun in different wavelengths and features of the sun (sunspot)

They appear dark or black in colour due to the reduced surface temperature caused by concentrating magnetic flux that inhibit convection [17]. This strong magnetic field in the photosphere reduces the flux of energy from the Sun's interior, leading to a section of the surface that appears dark against the bright background of photospheric granules. The temperature of the umbra (the darkest region of a Sunspot) is approximately 3000–4500 K, which is significantly cooler than the rest of the surface which is at about 5780 K [12], [16].

Sunspots appear within active regions on the Sun. These active regions also host other phenomena such as coronal loops, prominences [18], and reconnection events. Most Solar flares and coronal mass ejections originate in these magnetically active regions around visible Sunspot groupings. Sunspots typically appear in pairs of opposite magnetic polarity. The two main features of Sunspots are: Umbra and Penumbra (Figure 1). The central, darkest region of a Sunspot where the magnetic field is at its strongest and almost normal (90 degrees) to the Sun's surface, or photosphere is Umbra [19]. Penumbra is a brighter region that may completely or partially surround the umbra. The penumbra is composed of radially elongated structures known as penumbral filaments and has a more inclined magnetic field compared to the umbra. Within Sunspot groups, multiple umbrae may be surrounded by a single, continuous penumbra.

Sunspots can be individual or in a group, having a lifespan extending from a few days to a few months before eventually decaying. They can expand or contract in size, and can merge or divide to form larger or smaller Sunspots [16] as they move across the Sun's surface. Their size can vary widely, with diameters ranging from about 16 km to 160,000 km [20]. They may travel with different speeds depending on the differential rotation of the Sun. As the Sun is a hot ball of Plasma, its different layers have different rotation speeds, with equator rotating faster than the poles. When viewed from above the Sun's North Pole, it rotates counter-clockwise, completing a rotation in about 25 Earth days at the equator and about 34 Earth days at the poles.

Initially, Sunspots appear as small darkened spots without a penumbra, known as Solar pores [21]. Over time, these pores can increase in size, and a penumbra will begin to form when a pore reaches a diameter of about 3,500 km. The concept of the Sunspot number was developed by Rudolf Wolf affiliated with the Zürich observatory during the nineteenth century. The Sunspot series, as initiated by him, is called the Zürich or Wolf Sunspot number (WSN) series [12]. The number of Sunspots varies based on the approximately 11-year Solar cycle. During this cycle, Sunspot populations tend to increase to an upper limit called the Solar maximum and then decrease to a lower limit called the Solar minimum. Early on in the cycle, Sunspots appear at higher latitudes and then move towards the equator as the cycle progresses, following the Spörer's law. Spörer's law describes the equatorward drift of average Sunspot latitudes during the 11-year Solar cycle. It essentially states that Sunspots initially appear at higher latitudes near 30-45 degrees and gradually move towards the Sun's equator as the cycle progresses. The Solar cycle is also linked to variations polarity of the Solar magnetic field within this period. George Ellery Hale first linked the magnetic fields of the Sun and the Sunspots and suggested a 22-year magnetic cycle involving polarity reversals.

The formation of Sunspots is a complex process that is still an area of active research, but the generally accepted understanding is that Sunspots are visible manifestations of magnetic flux tubes in the Sun's convective zone projecting through the photosphere within active regions. The Sun's magnetic field is generated by a dynamo process within its interior. This process creates strong, concentrated bundles of magnetic field lines known as magnetic flux tubes within the convective zone.

The Solar Dynamics Observatory (SDO) is a NASA mission with an Earth-orbiting Solar telescope that provides high-resolution images of the Sun in various wavelengths [22]. This sky-observatory is launched to study the different parameters of the Sun and get detailed Heliophysical data [22], [23].

In the present study, an attempt has been made to study the features and dynamics of Sun. This includes the study of dynamics of Sunspots and applying the machine-learning techniques on observational data. Polynomial regression models in Python have been employed to predict the motion of Sunspots over time, enabling us to estimate when a Sunspot would complete a Solar rotation and reappear on the visible disk. By calculating the velocity of Sunspots from distance and time data, the kinematics of sunspots are analysed. The variation in Sunspot area was also analysed, although it was found to be more complex due to the need for additional factors like magnetic field and polarity data. Additionally, a pre-trained model (OpenCV library) to count the number of Sunspots over time has been implemented, and temperature mapping of the solar surface from HMIIC filter images from SDO has been done. These objectives are proposed to act as a bridge connecting observational study of Sun and machine-learning techniques to analyze it.

The applications of this project are significant in space weather forecasting, as understanding Sunspot dynamics is crucial for predicting Solar flares and geomagnetic storms that can impact satellite communication, navigation systems, and power grids on Earth. This blend of observational astronomy and analytical modeling not only deepened our understanding of Solar activity but also highlighted the importance of integrating data science with Astrophysics.

Several studies have delved into the nature and behavior of sunspots, which are dark regions on the solar surface linked to intense magnetic activity. One study uses SDO data of Sun to detect and study Sunspots using Mathematical Morphology method [24]. One study also detects the Sunspots, but it uses a deep learning model which automatically detects sunspots from MDI and HMI image datasets [25]. Another study uses OpenCV methods in python to detect the sunspots and track them [16]. Some studies show about the SDO and their different types of data, images and instruments [17], [26]. One uses digital images captured by two telescopes at the Mitaka campus of the National Astronomical Observatory of Japan to study and measure sunspots area using automated sunspot detection. Their study gives high correlation and the ease of calibrating area discrepancies with a correction factor, their automated sunspot detection appears promising for future sunspot-area measurements [27], meanwhile, one of the studies investigates the relationship between the rotation of Sunspots and magnetic flux tubes [28]. Another study aims to determine a number of sunspot properties over cycle 23, mainly focuses on their distribution on the solar disk, maximum magnetic field and umbral/penumbral areas [29]. Another study includes kinetic plasma physics of the solar corona and solar wind. They explain kinetic aspects of plasma through Landau- and cyclotron-resonant damping of plasma waves [10]. Another study aims to study and explain existence of prominence, their stability and disappearance [18]. In a review paper titled "A history of solar activity over millennia", a qualitative information of past solar activity, over long times, was discussed [12].

II. Data and Analysis

A. SDO Data

Solar Dynamic Observatory (SDO) is the first mission and a part of NASA's Living with a Star (LWS) program. The program is aimed at understanding the causes of Solar variability and what impacts it has on Earth [22]. SDO exists to help us understand the Sun's influence on Earth and the space near it by studying the Solar atmosphere in small scales of space and time in multiple wavelengths simultaneously. SDO was launched on February 11, 2010, 10:23 am EST on an Atlas V from SLC 41 from Cape Canaveral [22], [23].

The main instruments of SDO are - Atmospheric Imaging Assembly (AIA), EUV Variability Experiment (EVE) and Helioseismic and Magnetic Imager (HMI) [22].

Each of these instruments perform several measurements that characterize how and why the Sun varies. These instruments are used to observe the Sun simultaneously, performing the entire range of measurements necessary to understand and record the variations on the Sun.

SDO is a Sun-pointing semi-autonomous spacecraft, which allows it to perform nearly continuous observations of the Sun [17], [26] with a continuous science data downlink rate of 130 Megabits per second (Mbps). The Solar Dynamics Observatory (SDO) represents a new frontier in quantity and quality of Solar data with a data of about 1.5 TB per day [17]. SDO's inclined geosynchronous orbit was chosen to allow continuous observations of the Sun and enable its exceptionally high data rate through the use of a single dedicated ground station [17], [26].

As the Sunspots appears on the, so-called, surface of the Sun, Photosphere, monitoring and recording this layer is essential to study the different features of Sun. In this study, we used images taken from the HMIIC filter — the Helioseismic and Magnetic Imager Intensity Continuum — onboard NASA's Solar Dynamics Observatory (SDO). These images represent the visible continuum light near the Fe I 6173 Å absorption line, a region of the spectrum formed in the lower photosphere. The HMI instrument uses a narrow-band filter with a spectral resolution of 75 milli angstroms (0.075 Å) to scan across the Fe I 6173 Å line. By capturing multiple images at slightly different wavelengths, the instrument is able to generate precise intensity maps of the Sun's surface [22]. These are then processed to derive four primary observables: (1) continuum intensity images (like HMIIC) used for visualizing features such as Sunspots and granulation [25], (2) Dopplergrams which map the line-of-sight velocity of plasma flows on the Sun, and (3) both line-of-sight and vector magnetograms that represent the strength and direction of the Sun's magnetic field. These datasets play a critical role in understanding Solar activity and are especially valuable for identifying and analysing Sunspots, which are regions of concentrated magnetic activity [22].

B. Reference Points Values

The images downloaded from SDO are of same size, i.e. 1024 x 1024 pixels [17], [22], [26]. Thus, to measure the distance in each image, a reference value or scale is required. Also, the reference value or scale should be such that it minimizes the error encountered when measurement is done at or from the limbs (edges) of the Sun. So, the diameter of the Sun seen in the image is taken half of the Circumference of the Sun is noted as the reference value/scale, i.e., 2,189,500 km.

Using the AstroImageJ software, the solar diameter (from the left to the right limb) was selected with the "Line Tool" and assigned a real-world value of 2,189,500 km via the "Set Scale" option. This calibration established a reference scale, where 963.34 pixels, corresponding to the Sun's apparent diameter in the image, equaled 2,189,500 km. Accordingly, the pixel-to-kilometer conversion was calculated as approximately 4.40×10^{-4} pixels/km, or conversely, about 2,272.73 km/pixel. This reference scale was uniformly applied for all subsequent measurements performed on solar images captured between January 2025 and March 2025.

To measure the distance of individual Sunspots, an additional reference direction and origin point were established. Given that the Sun rotates in a counterclockwise direction (from east to west) when observed from above its northern pole, the apparent motion of Sunspots follows this same east-to-west trajectory. Therefore, distance measurements were consistently conducted from the Sun's eastern limb (left edge) to the centroid of the Sunspot, maintaining a left-to-right orientation within each image frame

C. Sunspots Distance Prediction Model

This study aims to monitor and predict the positional evolution of Sunspots over time using a combination of high-resolution solar imagery and data-driven modeling. A representative Sunspot, denoted as S1, was selected and tracked as it traversed the solar disk until reaching the western limb or disappearing behind the Sun's visible horizon. The tracking interval typically spanned approximately 7 days, although this duration varied depending on the Sunspot's lifespan and angular velocity.

The fundamental objective was to quantify the Sunspot's displacement relative to the Sun's eastern limb and apply these measurements to develop a predictive model of its motion, guided by the rotational dynamics of the Sun.

Solar observations were sourced from the Helioseismic and Magnetic Imager (HMI) aboard NASA's Solar Dynamics Observatory (SDO). Each image was captured at 1024 × 1024 pixels resolution, with a temporal cadence of one hour. Utilizing AstroImageJ, a line was drawn from the eastern limb of the solar disk to the Sunspot's centroid using the "Line Tool." This line's length, interpreted via the pre-established scale, was recorded in kilometers for each image in which Sunspot S1 remained visible.

To model the Sunspot's motion, a polynomial regression algorithm was implemented in Python. This supervised machine learning technique was employed to fit a nonlinear mathematical function to the observed distance-versus-time data. The model was trained to recognize the Sunspot's translational pattern across the solar disk and was then used to extrapolate future positions. Polynomial regression was selected for its ability to accurately represent nonlinear trajectories, making it well-suited for modeling Sunspots' movement on the rotating solar photosphere. All the sunspots that were tracked during january to march are given in the Table 2.

This predictive approach has broader implications. It facilitates the forecasting of Sunspot reappearances, enables estimation of solar rotation rates, and enhances understanding of the dynamics within active solar regions.

TABLE II. SUNSPOT TRACKING SUMMARY (JAN-MAR 2025)

Sunspot	**Tracking date**		
	Start	***End***	***Remark***
JAN-S1	14-01-2025	21-01-2025	Initial appearance
JAN-S1	01-02-2025	07-02-2025	Reappears after rotation
FEB-S2	12-02-2025	17-02-2025	New sunspot
MAR-S3	10-03-2025	16-03-2025	New sunspot
MAR-S4	13-03-2025	19-03-2025	New sunspot

D. Sunspots Area Variations

The growth and decay of Sunspots were systematically analyzed by monitoring changes in their projected area over time. A representative Sunspot, hereafter referred to as S1, was selected and tracked across the visible solar disk until it either reached the western limb or became obscured beyond the Sun's visible horizon. The tracking duration generally spanned approximately 7 days, although this interval varied depending on the Sunspot's lifetime and rotational velocity. The primary objective was to

quantify the temporal variation in the area of S1 and predict its subsequent growth or decay, a phenomenon intrinsically linked to the magnetohydrodynamic dynamics of the Sun.

To perform the measurements, high-resolution (1024 × 1024 pixels) images of the solar photosphere were obtained at one-hour intervals. These images were acquired from the Helioseismic and Magnetic Imager (HMI) onboard NASA's Solar Dynamics Observatory (SDO). Image processing and analysis were conducted using AstroImageJ, a robust astronomical image analysis software. The "Polygon Tool" within the software was employed to delineate the contour of the Sunspot in each frame as it progressed across the visible solar disk. The enclosed area was then computed in square kilometers, using a previously calibrated spatial reference scale. This process was repeated for all images in which Sunspot S1 was visible.

To model the temporal behavior of the Sunspot's area, a polynomial regression model was developed using the Python programming environment. This supervised machine learning technique was trained on the series of observed area values to derive a mathematical function that characterizes the nonlinear relationship between time and area variation. The trained model was subsequently used to extrapolate future area values, thereby providing predictions of continued Sunspot evolution.

Polynomial regression was chosen for its ability to effectively model nonlinear temporal trends, making it particularly well-suited for describing the complex morphological evolution of Sunspots on a rotating and dynamically active solar surface.

This predictive framework offers valuable insights into the magnetic activity cycles of the Sun, the formation and dissolution of active regions, and contributes to the broader understanding of solar variability and space weather phenomena.

E. Sunspots Velocity Variations

The Sun, being a massive sphere of high-temperature plasma, lacks a solid surface like terrestrial planets. Consequently, its various internal and surface layers rotate at different angular velocities, resulting in a phenomenon known as differential rotation. This differential motion induces shearing and twisting of magnetic field lines at the solar surface, contributing to the complexity of the Sun's magnetic topology. Understanding the mechanics of differential rotation is therefore essential for interpreting a wide range of solar phenomena, including the generation, evolution, and monitoring of magnetic fields [28].

Sunspots, which are visible manifestations of magnetic activity on the photosphere, exhibit motion that reflects the underlying differential rotation. Different Sunspots often move at distinct velocities, a behavior attributed to the varying rotational speeds of the latitudinal bands in which they are embedded.

By utilizing the Sunspot distance data, along with the corresponding time intervals over which these positions were recorded, the linear velocity of each Sunspot can be calculated. Since Sunspots located at different solar latitudes exhibit varying angular velocities, tracking their motion serves as a diagnostic tool for studying the Sun's differential rotation.

This analysis contributes to a deeper understanding of the rotational dynamics of the Sun, particularly how surface features like Sunspots trace the plasma flow patterns and provide insight into the Sun's internal rotation profile. The following equation to calculate the velocity of each Sunspot from JAN-S1 to MAR-S4:

$$v = \frac{(x_2 - x_1)}{(t_2 - t_1)} \qquad \square\square\square$$

Where v is velocity and x_2, x_1 and t_2, $t_1$are distances and time respectively.

From the distance data of each Sunspot, their respective velocity is calculated using the above equation in python. These velocities were recorded and plotted against time. The time here is taken as given in the below equation:

$$t = \frac{(t_2 + t_1)}{2} \qquad \square\square\square$$

Using these equations, velocity is calculated and then plotted against time for each Sunspot from JAN-S1 to MAR-S4. Thus, we get the velocities of different layers of the Sun which led us to the study of differential rotation of the Sun.

F. Number Of Sunspots

The quantification of Sunspots serves as a reliable proxy for monitoring solar activity and assessing space weather conditions [16], [24]. Periods of elevated Sunspot counts, referred to as solar maxima, are associated with increased probabilities of solar flares and coronal mass ejections (CMEs). Conversely, during periods of minimal Sunspot activity—solar minima—the Sun exhibits lower levels of magnetic activity, which may result in enhanced cosmic ray penetration into Earth's atmosphere due to the reduced solar magnetic shielding.

An OpenCV-based image processing pipeline was implemented to automatically detect and count Sunspots in sequential HMIIC filtergrams obtained from NASA's Solar Dynamics Observatory (SDO). OpenCV, an open-source computer vision and machine learning library, provides over 2,500 optimized algorithms capable of executing tasks such as object recognition, motion tracking, and image segmentation [16]. This framework was selected for its efficiency and robustness in identifying solar features such as Sunspots.

Images were acquired at hourly intervals from January to March, covering approximately three months. Each image was loaded using the cv2.imread function and converted to RGB format for visual representation and preprocessing. Due to the presence of a timestamp in the lower-left corner of each image, the bottom 50 pixels were cropped to eliminate potential interference during feature extraction. The image was then converted to grayscale, given that Sunspot detection is largely dependent on intensity gradients.

To suppress image noise while preserving critical edge details, a median blur filter (cv2.medianBlur) was applied. This was followed by adaptive Gaussian thresholding (cv2.adaptiveThreshold), which dynamically adjusts threshold values across local

regions of the image, thereby effectively isolating darker Sunspot areas from the surrounding brighter solar photosphere. A circular mask was then applied to focus detection solely within the solar disk, excluding the background.

Potential Sunspot regions were identified using contour detection (cv2.findContours). Only external contours within a predefined area range (20–7000 pixels) were considered valid Sunspot candidates. This range was determined empirically to minimize false positives arising from noise or irrelevant features. Detected contours were overlaid on the images for verification, and the count of validated Sunspots was recorded.

The extracted data were saved in CSV format, enabling quantitative analysis. A scatter plot was generated in Python to represent the Sunspot count as a function of time (in hours) over the three-month observation period. This automated and scalable method provides a powerful tool for monitoring solar activity trends, contributing to real-time space weather forecasting and advancing the understanding of the solar cycle.

G. Mapping the Photospheric Temperature Distribution of the Sun Using HMIIC Data

Monitoring the temperature distribution of the Sun is fundamental to understanding the various physical phenomena occurring within and across its layers. The core of the Sun attains temperatures of approximately 15 million kelvins, while the outer visible layer—the photosphere—maintains an average temperature near 5,773.15 K. In contrast, Sunspots, which are localized magnetic features on the photosphere, exhibit significantly cooler temperatures, generally ranging between 3,000 K and 4,500 K. Consequently, spatially resolving temperature variations across the solar surface offers critical insights into solar dynamics and magnetic activity.

Helioseismic and Magnetic Imager Intensity Continuum (HMIIC) images from NASA's Solar Dynamics Observatory (SDO) were utilized to generate a temperature map of the Sun's photosphere. The objective was to visualize thermal variations across the solar disk by employing an intensity-to-temperature mapping technique based on known reference temperatures.

To achieve this, the upper temperature limit was set as T_{max} = 5773.15 K (the typical photospheric temperature), and the lower limit was taken as T_{min} = 3700 K, representative of the average temperature of Sunspots. A linear mapping method was then applied to the pixel intensity values in the grayscale images, transforming these intensities into corresponding temperature values within the defined range. This technique assumes a monotonic relationship between image brightness and temperature, enabling a pixel-wise estimation of surface temperature.

The resulting temperature map allowed for the visualization of thermal gradients across the photosphere. Cooler regions, corresponding to Sunspots, were distinctly visible, contrasted against the warmer background of the ambient photosphere. This analysis facilitates a detailed thermal characterization of solar surface features, offering valuable information about local magnetic phenomena, energy transport, and surface convection dynamics.

This methodology not only enhances our understanding of the Sun's thermal behavior but also contributes to broader efforts in space weather forecasting and the study of magnetohydrodynamic processes within stellar environments.

III. RESULTS

A. Sunspot Distance Analysis

The Sunspot JAN-S1 was tracked from 14 January 2025 at 00:00:00 to 21 January 2025 at 23:00:00 as shown in Figure 2, and its motion across the solar disk was recorded. In Figure 3, the observed distances are shown in blue, while the predicted values from a polynomial regression model appear in green. A red marker indicates the predicted time at which the Sunspot completes one full rotation and returns to its original position.

The model forecasted that JAN-S1 would complete its solar rotation in 388.58 hours, corresponding to 30 January 2025 at 04:00:00. This prediction was confirmed through image verification at the specified time, validating the model's accuracy in predicting solar rotation based on Sunspot tracking.

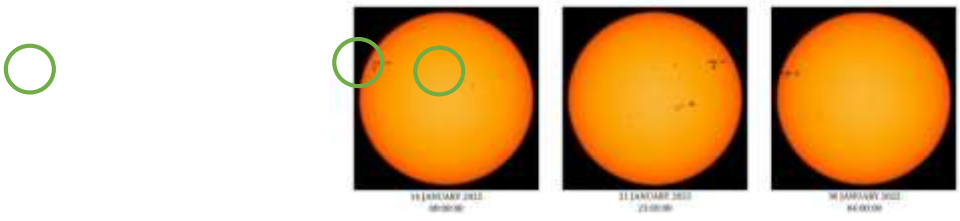

Fig. 2. The movement of the Sunspot "JAN-S1" with date and time.

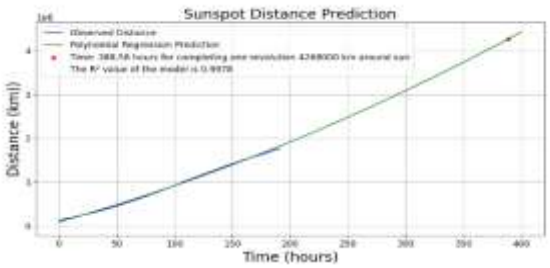

Fig. 3. Distance vs. Time plot for observed and predicted distances of the Sunspot "JAN-S1".

Due to its sustained size, Sunspot JAN-S1 was tracked again from 01 February 2025 at 06:00:00 to 07 February 2025 at 23:00:00, with time reset to 0 hours (Figure 5).

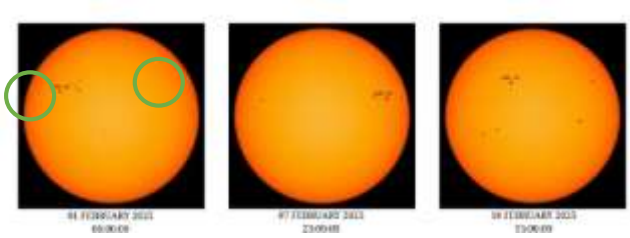

Fig. 4. The movement of the Sunspot "JAN-S1" with date and time.

Fig. 5. Distance vs. Time plot for observed and predicted distances of the Sunspot "JAN-S1" as it is further tracked.

Based on this second tracking period, the model predicted that the Sunspot would complete another full rotation at 423.44 hours, corresponding to 18 February 2025 at approximately 15:00. This prediction was visually confirmed using the image taken at 18 February 2025, 15:00:00 (Figure 4), validating the model's reliability in forecasting solar rotation cycles.

Sunspot JAN-S1 was further tracked from 17 February 2025 at 00:00:00 to 22 February 2025 at 23:00:00, with time reset to zero. The model predicted that the Sunspot would complete its second full rotation at 395.28 hours (Figure 7), corresponding to 5 March 2025 at approximately 11:00. However, by the predicted time, the Sunspot had shrunk in size, and no Sunspot was observed in the region, suggesting it had completely vanished before completing its second rotation (Figure 6).

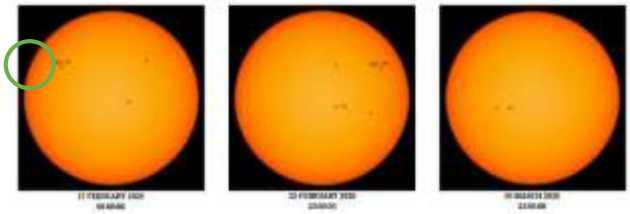

Fig. 6. The movement of the Sunspot "JAN-S1" with date and time.

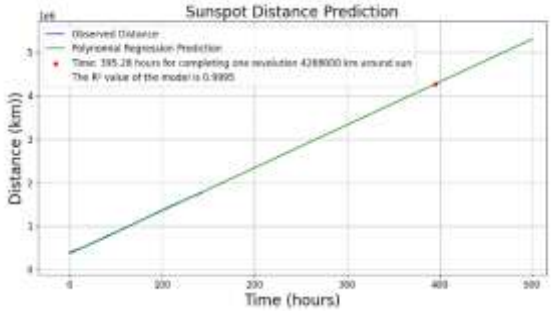

Fig. 7. Distance vs. Time plot for observed and predicted distances of the Sunspot "JAN-S1".

FEB-S2 was tracked from 12 February 2025 at 00:00:00 to 17 February 2025 at 23:00:00 (Figure 8). The model predicted that it would complete one full rotation at 380.47 hours, corresponding to 27 February 2025 at approximately 20:00 (Figure 9). This prediction was confirmed with the observed image of 27 February 2025 at 20:00:00. However, the Sunspot was not tracked further as it nearly vanished before reaching the rightmost edge on 3 March 2025.

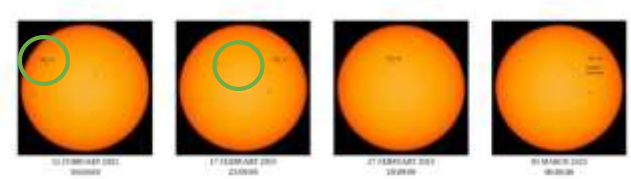

Fig. 8. The movement of the Sunspot "FEB-S2" with date and time.

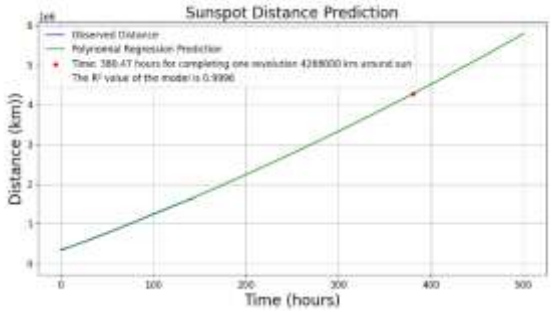

Fig. 9. Distance vs. Time plot for observed and predicted distances of the Sunspot " FEB-S2".

MAR-S3 was tracked from 10 March 2025 at 00:00:00 to 16 March 2025 at 23:00:00 (Figure 10). The model predicted that it would complete one full rotation at 445.01 hours, corresponding to 28 March 2025 at approximately 13:00 (Figure 11).

Fig. 10. The movement of the Sunspot "MAR-S3" with date and time.

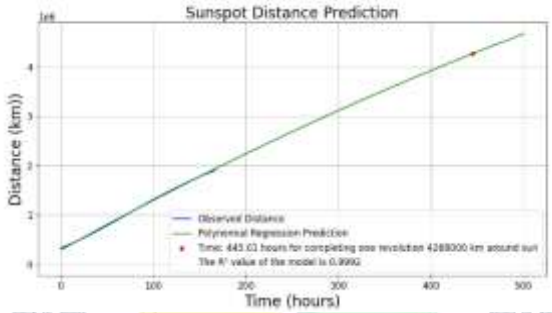

Fig. 11. Distance vs. Time plot for observed and predicted distances of the Sunspot " MAR-S3".

However, as the Sunspot was small in size and nearing the rightmost edge on 16 March 2025, it likely vanished before completing its rotation, as no Sunspot was observed in the predicted region at the specified time.

The fourth Sunspot, MAR-S4 was tracked from 13 March 2025 at 00:00:00 to 19 March 2025 at 23:00:00 (Figure 12). The model predicted that it would complete one full rotation at 433.23 hours, corresponding to 31 March 2025 at approximately 01:00 (Figure 13). This prediction was confirmed with the observed image on 31 March 2025 at 01:00:00.

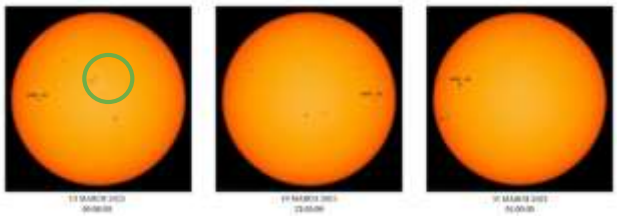

Fig. 12. The movement of the Sunspot "MAR-S4" with date and time.

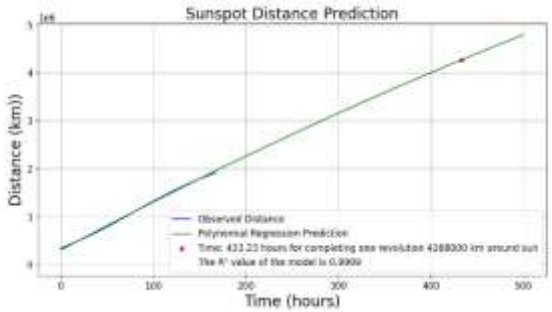

Fig. 13. Distance vs. Time plot for observed and predicted distances of the Sunspot " MAR-S4".

B. Sunspot Area Variations

The area of Sunspot "JAN-S1" was measured using AstroImageJ with the initial scale. The measured data was fed into the model, and predictions are shown in Figure 14. The plot represents a second-degree polynomial distribution of observed and predicted values over time. The R^2 value of the model, calculated using SKLEARN in Python, was 0.945.

The observed distance is marked in blue, while the predicted future distance is in green. The red mark indicates the time when the area is predicted to become zero. The model predicts this occurs at 263 hours, but reappearance was observed on 30 January 2025 (Figure 2), suggesting additional factors influence Sunspot area and their growth/decay.

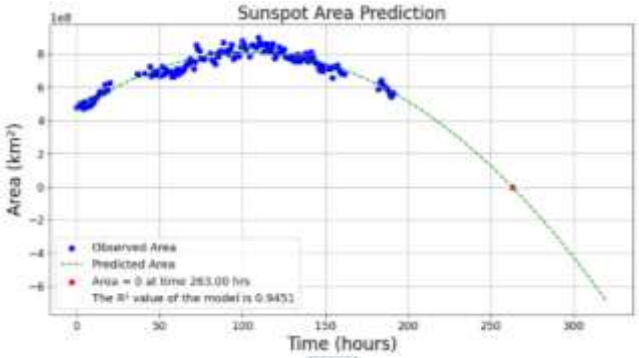

Fig. 14. The area prediction for sunspot "JAN-S1"

C. Sunspot Velocity Calculation

Using the data collected for the distance model, the velocity of each Sunspot at different latitudes are calculated. This, in turn, gives the velocity of different latitudes of the Sun in photosphere.

For the first Sunspot “JAN-S1”, using its observed distances over the time from 14th January 2025 at 00:00:00 to 21st January 2025 at 23:00:00, its velocity is calculated and plotted against time using Matplot library in python. The resultant graph is shown in Figure 15. The average velocity of Sunspot “JAN-S1” was 8897.47 km/hr which is represented by red line. Its velocity varies from about 2500 km/hr to about 20000 km/hr.

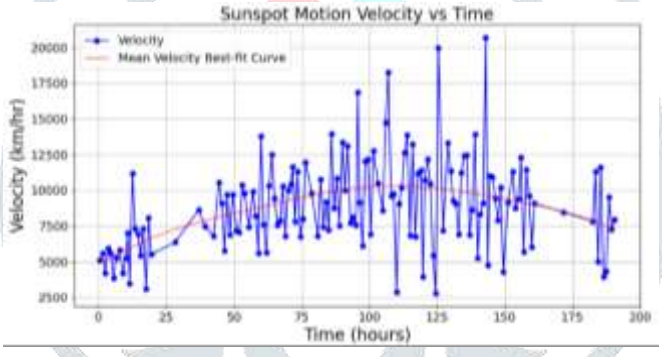

Fig. 15. Velocity vs. time plot for sunspot "JAN-S1"

This velocity increases gradually from when it was first observed or originated to when it reaches the right most edge. However, we can also see from the graph that the velocity isn’t steady and varies rapidly with time. The same sunspot observed from 01st February 2025 at 06:00:00 to 07th February 2025 at 23:00:00 and later from 17th February 2025 at 00:00:00 to 22nd February 2025 at 23:00:00 shows mean velocity of 9705.93 km/hr and 9552.23 km/hr respectively, which shows that velocity of the sunspot varies non linearly with time. The velocity calculations for the sunspots observed in february and march are given in the Table 3.

TABLE III. VELOCITY CALCULATIONS FOR THE OBSERVED SUNSPOTS

Sunspot	**Velocity (km/hr)**	
	Average velocity	***Range***
JAN-S1	8897.47	~2500 to 20000
FEB-S2	9095.20	~00 to 17500
MAR-S3	9428.59	~2000 to 16000
MAR-S4	9446.87	~4000 to 14000

D. Number Of Sunspots

The number of Sunspots were counted in each image at an interval of one hour from 14th January 2025 at 00:00:00 to 31st March 2025 at 23:00:00. The data was plotted using Matplotlib in Python, as shown in Figure 16. Blue dots represent observed counts, and green lines connect the data points. This graph illustrates variations in visible Sunspots over time, reflecting changes in Solar activity—higher counts correspond to increased activity, and lower counts indicate reduced activity.

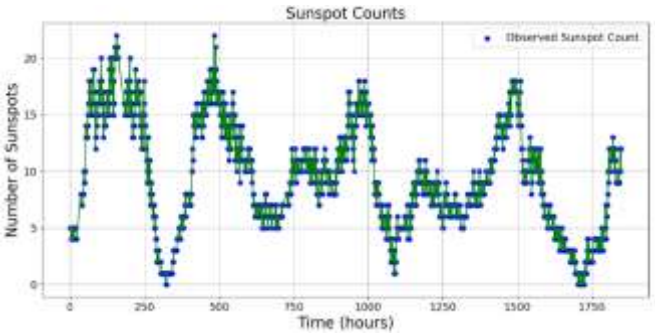

Fig. 16. Number of sunspots from 14th january 2025 to 31st march 2025 against time.

As the Sunspots are the surface phenomena occurs on the Sun's photosphere, the number of Sunspots visible can be related to the Solar activity. The higher the number of Sunspots, more will be the Solar activity. Similarly, lower the number of Sunspots, less will be its activity. From the graph, it can be seen that the pattern is similar to trigonometric Sine or Cosine function, i.e., the number of Sunspots over time increases and decreases similar to trigonometric Sine or Cosine function. There were peaks when Solar activity is maximum and number of Sunspots was seen to be around 20-25, whereas, during the depths when Solar activity was minimum, the number of Sunspots were around 0-5.

E. Temperature mapping of the Sun

A linear mapping was applied to convert image intensity values into temperature values within the range T_{max} = 5773.15 K and T_{min} = 3700 K. This mapping was performed on each HMIIC image from SDO between 14 January 2025 and 31 March 2025.

20 JAN 2025

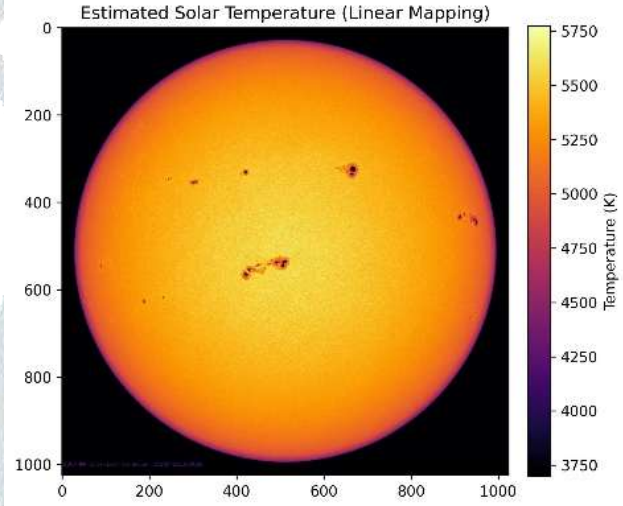

20 FEB 2025

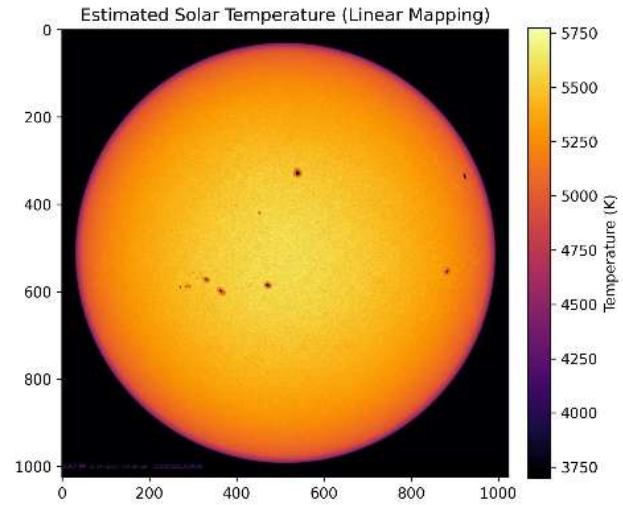

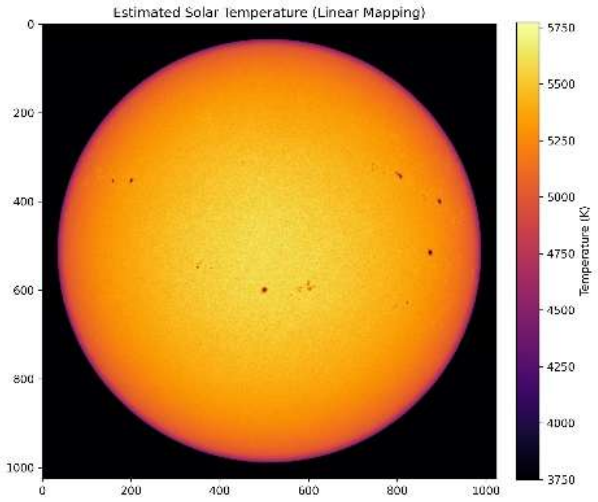

Fig. 17. Temperature mapping examples for Sun for 20th january, 20th february 2025 and 20th march 2025.

The resulting temperature maps as shown in Figure 17 enable detailed analysis of the Sun's photospheric temperature, revealing spatial and temporal variations essential for studying Solar surface dynamics.

IV. CONCLUSIONS

The developed distance prediction model effectively forecasted the movement of Sunspots across the solar disk and accurately predicted the time and date at which a Sunspot would complete one full rotation and return to its original position. The model is based on second-degree polynomial regression, which captures the trend in spatial movement over time. These results indicate that the motion of individual Sunspots follows a quadratic trend, though the specific polynomial may vary across different Sunspots.

The area of a Sunspot was modeled using polynomial regression to estimate its future size variation over time. However, the model's predictions showed deviations from actual observations, suggesting that Sunspot area is influenced by additional complex factors. These include solar magnetic field strength, magnetic polarity, Sunspot merging or fragmentation, and possibly other dynamic solar surface phenomena. Therefore, accurate area prediction requires the inclusion of these contributing factors. Velocity analysis revealed that Sunspots move at different speeds depending on their latitude. It was observed that Sunspots near the equator exhibit higher velocities, while those at higher latitudes move more slowly. This confirms the differential rotation of the Sun, consistent with its plasma nature. The findings support the conclusion that the Sun's angular velocity decreases with increasing latitude. The temporal variation in Sunspot count follows a periodic pattern resembling sine or cosine functions. This fluctuation reflects changes in solar activity, with higher Sunspot numbers indicating heightened activity. The analysis showed a peak in activity around January 2025, followed by a gradual decline toward March 2025. This trend suggests a possible increase in activity in subsequent months, aligning with the cyclical nature of the solar magnetic cycle. Daily linear temperature mapping from January to March 2025 shows that the surface temperature of the Sun can be effectively visualized using image intensity scaling in Python. Individual temperature values across the solar disk can be monitored, with improved accuracy achievable through better estimates of minimum and maximum temperature limits. The observed limb darkening effect, wherein intensity and thus apparent temperature decrease toward the solar limb, was consistent with theoretical expectations. This mapping facilitates a deeper understanding of photospheric temperature distribution and temporal evolution, as well as validation of solar optical phenomena such as limb darkening.

ACKNOWLEDGMENT

The authors gratefully acknowledge the Solar Dynamics Observatory (SDO) and the National Aeronautics and Space Administration (NASA) for providing continuous and invaluable access to a comprehensive database of high-resolution solar images across multiple wavelengths. The daily availability of these datasets has been instrumental in facilitating this research. The support and contributions of all individuals involved in maintaining these observational missions are sincerely appreciated.

REFERENCES

[1] Gough D. (1983) Our first inferences from helioseismology. *Phys. Bull.* **34**, 502–507. (doi:10.1088/0031-9112/34/12/019)

[2] Connelly J.N., Bizzarro M., Krot A.N., Nordlund Å., Wielandt D. & Ivanova M.A. (2012) The absolute chronology and thermal processing of solids in the solar protoplanetary disk. *Science* **338**, 651–655. (doi:10.1126/science.1226919)

[3] Falk S.W., Lattimer J.M. & Margolis S.H. (1977) Are supernovae sources of presolar grains? *Nature* **270**, 700–701. (doi:10.1038/270700a0)

[4] Woolfson M. (2000) The origin and evolution of the solar system. *Astron. Geophys.* **41**, 1.12–1.19. (doi:10.1046/j.1468-4004.2000.00012.x)

[5] Charity M. What color are the stars? - some pixel RGB values.

[6] Soriano M. & Vauclair S. (2010) New seismic analysis of the exoplanet-host star μ Arae. *Astron. Astrophys.* **513**, A49. (doi:10.1051/0004-6361/200911862)

[7] Williams D.R. Sun Fact Sheet. Accessed 15 Apr 2025. Available online: https://nssdc.gsfc.nasa.gov/planetary/factsheet/sunfact.html

[8] Harvey S. Solar System Exploration. Accessed 15 Apr 2025. Available online: https://web.archive.org/web/20080102034758/http://solarsystem.nasa.gov/planets/profile.cfm?Object=Sun&Display=Facts&System=Metric

[9] Prša A. *et al.* (2016) Nominal values for selected solar and planetary quantities: IAU 2015 Resolution B3. *Astron. J.* **152**, 41. (doi:10.3847/0004-6256/152/2/41)

[10] Marsch E. (2006) Kinetic physics of the solar corona and solar wind. *Living Rev. Sol. Phys.* **3**, 1. Available online: http://www.livingreviews.org/lrsp-2006-1

[11] Christian E.R. Ask Us Sun. Accessed 15 Apr 2025. Available online: https://web.archive.org/web/20180903223810/https://helios.gsfc.nasa.gov/qa_sun.html#negative

[12] Usoskin I.G. (2017) A history of solar activity over millennia. *Living Rev. Sol. Phys.* **14**, 1. (doi:10.1007/s41116-017-0006-9)

[13] Abhyankar K.D. Abhyankar. Centre of Advanced Study in Astronomy, Osmania University, Hyderabad 500007.

[14] Prša A. *et al.* (2016) Nominal values for selected solar and planetary quantities: IAU 2015 Resolution B3. *Astron. J.* **152**, 41. (doi:10.3847/0004-6256/152/2/41)

[15] Discovery of Helium. Accessed 15 Apr 2025. Available online: https://web.archive.org/web/20151107043457/http://www-solar.mcs.st-andrews.ac.uk/~clare/Lockyer/helium.html

[16] Du Toit R., Drevin G., Maree N. & Strauss D.T. (2020) Sunspot identification and tracking with OpenCV. In *2020 Int. SAUPEC/RobMech/PRASA Conf.* (doi:10.1109/SAUPEC/RobMech/PRASA48453.2020.9040971)

[17] NOAA National Weather Service. Space Weather Prediction Center. Accessed 15 Apr 2025. Available online: https://www.swpc.noaa.gov/phenomena/solar-cycle

[18] Hathaway D.H. (2010) The solar cycle. *Living Rev. Sol. Phys.* **7**, 1. (doi:10.12942/lrsp-2010-1)

[19] Owens M.J. & Forsyth R.J. (2013) The heliospheric magnetic field. *Living Rev. Sol. Phys.* **10**, 5. (doi:10.12942/lrsp-2013-5)

[20] Riley P., Lionello R., Linker J.A. & Mikic Z. (2012) Corotating interaction regions during the recent solar minimum: The power and limitations of global MHD modeling. *J. Atmos. Sol.-Terr. Phys.* **83**, 1–10. (doi:10.1016/j.jastp.2011.12.013)

[21] Howard R.A. *et al.* (1982) Initial SOHO observations of coronal mass ejections. *Astrophys. J.* **263**, L101–L104. (doi:10.1086/183932)

[22] Harrison R.A., Davies J.A., Biesecker D.A., Gibbs M., Perry C.H. & Waltham N.R. (2018) The STEREO mission: An overview. In *The Sun, the Solar Wind, and the Heliosphere* (eds. M. Dryer & N. Meyer-Vernet), pp. 135–176. Springer, Dordrecht. (doi:10.1007/978-94-007-2732-3_7)

[23] Baker D.N. *et al.* (2008) Severe space weather events—Understanding societal and economic impacts. *Workshop Report*, National Academies Press, Washington, DC.

[24] Schrijver C.J. *et al.* (2015) Understanding space weather to shield society: A global road map for 2015–2025 commissioned by COSPAR and ILWS. *Adv. Space Res.* **55**, 2745–2807. (doi:10.1016/j.asr.2015.03.023)

[25] Love J.J., Hayakawa H., Cliver E.W., Humphries T., Owens M.J. & Riley P. (2019) On the intensity of the magnetic storm of 1–2 September 1859. *Space Weather* **17**, 1281–1292. (doi:10.1029/2019SW002250)

[26] Cliver E.W. & Dietrich W.F. (2013) The 1859 space weather event revisited: Limits of extreme activity. *J. Space Weather Space Clim.* **3**, A31. (doi:10.1051/swsc/2013053)

[27] Odenwald S. & Green J. (2008) Bracing the satellite infrastructure for a solar superstorm. *Sci. Am.* **299**, 80–87. (doi:10.1038/scientificamerican0808-80)

[28] Pulkkinen A. *et al.* (2017) Geomagnetically induced currents: Science, engineering, and applications readiness. *Space Weather* **15**, 828–856. (doi:10.1002/2016SW001501)

[29] Eastwood J.P. *et al.* (2017) The economic impact of space weather: Where do we stand? *Risk Anal.* **37**, 206–218. (doi:10.1111/risa.12765)